Proceedings of the 13th
KACC, October 1998

NEW MODELING AND CONTROL OF AN ASYMMETRIC HYDRAULIC ACTIVE SUSPENSION SYSTEM

Wanil Kim,* and Sangchul Won*

* Dept. Electr. Engr., POSTECH
San 31 Hyoja-Dong, Pohang 790-784, Korea
Tel: +82-562-279-2894
Fax: +82-562-279-8119
Email: sulchun@postech.ac.kr

Abstract

In this paper an asymmetric hydraulic actuator which consists of single acting cylinder and servo valve is modeled for a quarter car active suspension system. This model regards the force as an internal state rather than a control input. The control input of the model is the sum of oil flows that pass through the valve's orifices. The resulting dynamic equation in the state space appears a feedback connection of a nominal linear time invariant term with a nonlinear bounded uncertain block. Since this model makes it possible to eliminate the force control phase, analysis and controller design are made straightforward and simple. Well known LQR method is then applied. Simulation and test rig experiment show the effectiveness of this approach in modeling and control.

1. INTRODUCTION

During last three decades in the field of automotive active suspension design, extensive researches have been carried out to improve suspension quality which is mainly represented by ride comfort and road holding. Sky-hook control has a simple structure but is shown to be effective especially in ride comfort[1] and would be applied to a real car suspension[2]. Many other control methods like LQG, adaptive control and H_∞ were tried to to meet the such needs as the balance between the ride comfort and road holding, robustness against the uncertainty and so on[3–5]. Those methods assume that the actuator dynamics is so fast that any kind of force command can be generated correctly. A proportional type force control, however, is shown to require an ernormous feedback gain[6]. Alleyne and Hedrick applied an adaptive sliding mode control to the force control[7]. The conventional two step scheme, separate design of the ideal force command neglecting the actuator dynamics and the force controller including the actuator dynamics, seems complicated and the performance would be dependent on the specific force control.

In this paper a new quarter car model including the dynamics of an asymmetric hydraulic actuator is developed, which consists of a servo valve and a single acting cylinder suitable for limited package space. This model regards the actuator force as an internal state and the oil flow rate supplied by the valve as an control input. The dynamic equation is consists of a nominal linear time-invariant part and bounded parametric uncertainties. The new control scheme eliminates the unnecessary force control. As a result the analysis and controller design can be performed in a systematic way.

After the modeling of a quarter car with an asymmetric hydraulic actuator is given in Section 2, a single step control scheme is given and an optimal state feedback is applied as an example in Section 3. Simulation and test rig experiment results given and analyzed in Section 4. Concluding remarks follows in Section 5.

2. MODELING OF A QUARTER CAR

2.1 Asymmetric hydraulic actuator

The actuator considered in this paper is a combined asymmetric cylinder and a 4-way servo valve as shown in Fig. 1. Both the oil flow rates into and out of the cylinder are controlled by a single servo valve's spool motion, which is controlled by a solenoid. Following assumptions are employed:

- the servo valve dynamics is fast enough to be neglected.
- oil leakage and friction are negligible in the cylinder.
- the direction of oil flow is solely determined by the sign of the spool position, i.e. the supply pressure, P_s is sufficiently high so that reverse flow does not occur.

The pressure drop across the orifice $\Delta p_i (i = 1, 2)$ is defined as

$$\Delta p_1 = \begin{cases} P_s - p_1 & \text{if } v \geq 0 \\ p_1 - P_e & \text{if } v < 0 \end{cases} \quad (1)$$

$$\Delta p_2 = \begin{cases} p_2 - P_e & \text{if } v \geq 0 \\ P_s - p_2 & \text{if } v < 0 \end{cases} \quad (2)$$

Assuming the symmetry in the orifice geometries of the valve, the flow rate $q_i (i = 1, 2)$ via the orifices is

$$q_i = K_{eq} v \sqrt{\Delta p_i} \quad (3)$$

where v is an input voltage to the servo valve, K_{eq} is an equivalent gain of the valve. The sign of q_1 is

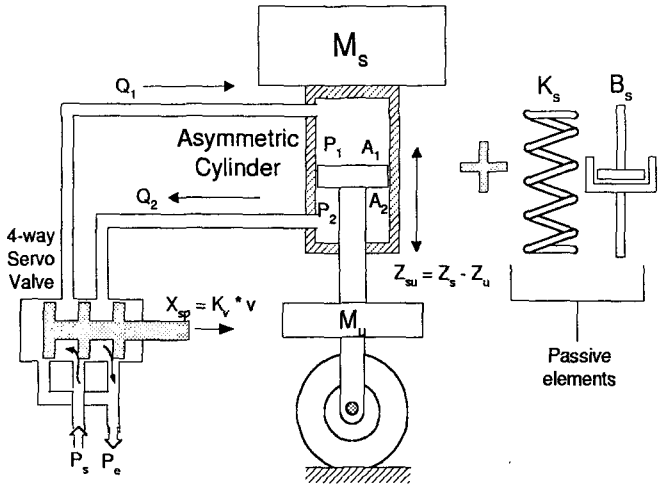

Fig. 1. Structure of the quarter car active suspension system

conventionally chosen positive when oil flows into the cylinder and negative when it does out of the cylinder. As for q_2, the convention is reversed.

From the continuity equation of fluid[8]

$$\begin{aligned} q_1 &= A_1\dot{z}_{su} + (V_1/B)\dot{p}_1 \\ q_2 &= A_2\dot{z}_{su} - (V_2/B)\dot{p}_2 \end{aligned} \tag{4}$$

where $A_i(i=1,2)$ is the piston area of each chamber and B is the bulk modulus of oil. The chamber volumes $V_i(i=1,2)$ is a function of cylinder stroke, $z_{su} \triangleq z_s - z_u(-L/2 \le z_{su} \le L/2)$

$$\begin{aligned} V_1(z_{su}) &= V_{10} + A_1 z_{su} \\ V_2(z_{su}) &= V_{20} - A_2 z_{su} \end{aligned} \tag{5}$$

where $V_{i0} = A_i(L/2 + l_i)$ is the neutral volume when $z_{su} = 0$, L is the length of the piston rod and l_i corresponds to a volume in the piping. With the piston area ratio, $\gamma \triangleq A_1/A_2(\gamma \ge 1)$, the load pressure is defined by

$$p_L \triangleq \gamma p_1 - p_2 \tag{6}$$

Then the force exerted by the cylinder is

$$f_a = A_1 p_1 - A_2 p_2 = A_2 p_L \tag{7}$$

Differentiating the both sides of (7) and rearranging (4), the cylinder equation is obtained.

$$\dot{f}_a = -B(\frac{A_1^2}{V_1} + \frac{A_2^2}{V_2})\dot{z}_{su} + B(\frac{A_1}{V_1}q_1 + \frac{A_2}{V_2}q_2) \tag{8}$$

The sum of the oil flow rate q_s by the servo valve is defined by

$$\begin{aligned} q_s &\triangleq q_1 + q_2 \\ &= K_{eq} v(\sqrt{\Delta p_1} + \sqrt{\Delta p_2}) \end{aligned} \tag{9}$$

Defining r_i for simplicity by

$$r_1 = \frac{\sqrt{\Delta p_1}}{\sqrt{\Delta p_1} + \sqrt{\Delta p_2}}, \quad r_2 = \frac{\sqrt{\Delta p_2}}{\sqrt{\Delta p_1} + \sqrt{\Delta p_2}} \tag{10}$$

and rearranging (8)

$$\dot{f}_a = \alpha(z_{su})\dot{z}_{su} + \beta(z_{su}, r_1, r_2)q_s \tag{11}$$

where

$$\alpha(z_{su}) \triangleq -B(\frac{A_1^2}{V_1(z_{su})} + \frac{A_2^2}{V_2(z_{su})}) \tag{12}$$

$$\beta(z_{su}, r_1, r_2) \triangleq B(\frac{A_1}{V_1(z_{su})}r_1 + \frac{A_2}{V_2(z_{su})}r_2) \tag{13}$$

Defining the nominal values, $\hat{\alpha}$ and $\hat{\beta}$ for $z_{su} = 0, \Delta p_1 = \Delta p_2 = (P_s - P_e)/2, (r_1 = r_2 = 1/2)$,

$$\hat{\alpha} \triangleq -\hat{B}(\frac{A_1^2}{V_1(0)} + \frac{A_2^2}{V_2(0)}) \tag{14}$$

$$\hat{\beta} \triangleq \frac{\hat{B}}{2}(\frac{A_1}{V_1(0)} + \frac{A_2}{V_2(0)}) \tag{15}$$

(11) is rewritten as

$$\dot{f}_a = \hat{\alpha}\dot{z}_{su} + \hat{\beta}[q_s + w_2(z_{su}, \dot{z}_{su}, r_1, r_2, q_s)] \tag{16}$$

where the model uncertainty is defined by

$$\begin{aligned} &w_2(z_{su}, \dot{z}_{su}, r_1, r_2, q_s) = \\ &\delta_1(z_{su})\dot{z}_{su} + \delta_2(z_{su}, r_1, r_2)q_s \end{aligned} \tag{17}$$

where $\delta_1(\cdot) = \hat{\beta}^{-1}(\alpha(\cdot) - \hat{\alpha})$ and $\delta_2(\cdot) = \hat{\beta}^{-1}(\beta(\cdot) - \hat{\beta})$. $w_2(\cdot)$ represents the uncertain parameters and the nonlinear dynamics of the hydraulic system. Typical behaviors of δ_1 and δ_2 are shown in Fig. 2.1 as a function of the piston stroke z_{su}. It is reasonable to assume that Δp_i's vary $\underline{p}$ to $\overline{p}$ causing

$$\underline{r} \le r_i \le \overline{r}, \quad i = 1, 2 \tag{18}$$

and z_{su} is bounded by $|z_{su}(t)| \le c$, $0 < c < L/2$ for safe operation. And the bulk moduls B is allowed to vary within $\pm 20\%$ of its nominal value. The effects of the uncertainty would be negligible if the actuator is operated around the mid-stroke.

We remark that the derived equations above are applicable to both symmetric and asymmetric types, but for symmetric one more simplification is possible owing to the equal piston areas. And the following symmetric equations hold during its whole operation.

$$P_s = p_1 + p_2, \quad p_L = p_1 - p_2 \tag{19}$$

2.2 State space description of a quarter car

The equations of motion for the quarter car in Fig. 3 are as follow.

$$M_s\ddot{z}_s = f_a \tag{20}$$

$$M_u\ddot{z}_u = -B_t(\dot{z}_u - \dot{z}_r) - K_t(z_u - z_r) - f_a \tag{21}$$

The tire is modeled as a parallel spring and damper. Note that passive elements such as spring and shock absorber are not included in this model, because their effects are overwhelmed by an active actuator if the supply pressure is chosen sufficiently high.

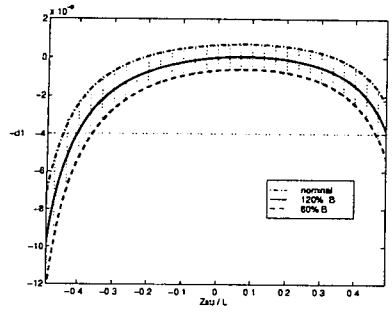

(a) δ_1

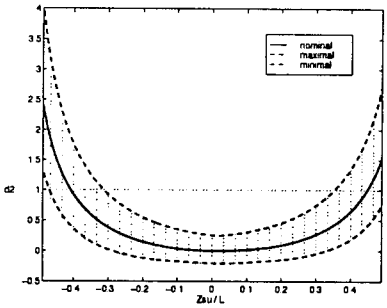

(b) δ_2

Fig. 2. Plot of δ_i when B varies within $\pm 20\%$ of B_{nom}

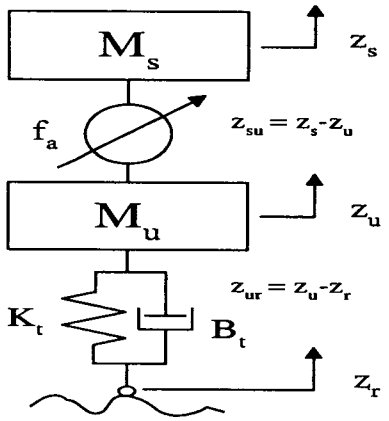

Fig. 3. Schematic diagram of a quarter car

Now the nominal state space equation is derived combining (21), (21) and the nominal part of (16).

$$\dot{\mathbf{x}} = \mathbf{A}\mathbf{x} + \mathbf{B_1}w_1 + \mathbf{B_2}u \tag{22}$$

where

$$\mathbf{x} = [\, z_s - z_u \;\; \dot{z}_s \;\; z_u - z_r \;\; \dot{z}_u \;\; f_a \,]^T,$$

$$w_1 = \dot{z}_r, \qquad u = q_s,$$

$$\mathbf{A} = \begin{bmatrix} 0 & 1 & 0 & -1 & 0 \\ 0 & 0 & 0 & 0 & 1/M_s \\ 0 & 0 & 0 & 1 & 0 \\ 0 & 0 & -K_t/M_u & -B_t/M_u & -1/M_u \\ 0 & \hat{\alpha} & 0 & -\hat{\alpha} & 0 \end{bmatrix},$$

$$\mathbf{B_1} = \begin{bmatrix} 0 \\ 0 \\ -1 \\ B_t/M_u \\ 0 \end{bmatrix}, \quad \mathbf{B_2} = \begin{bmatrix} 0 \\ 0 \\ 0 \\ 0 \\ \hat{\beta} \end{bmatrix}$$

Note in (22) that the active force belong to the state vector $\mathbf{x}$, control input is the sum of oil flow rates, q_s defined in (9). One can easily check that $(\mathbf{A}, \mathbf{B_2})$ pair is controllable.

The distribution of the eigenvalues of $\mathbf{A}$ based on the values in Table. 2, is compared with those of the passive system as follows.

Table 1. Eigenvalue Distribution

type	eigenvalues
passive	-2.15±8.46i, -24.48±57.84i
active	0, -1.35±23.22i, -7.60±1.05×10^3 i

The fact that the eigenvalue distribution is totally altered means that an active suspension system is not merely a supplement of an actuator parallel to a passive spring and damper.

3. CONTROLLER DESIGN

3.1 Single step control scheme

Conventional way of control of active suspension system generally consists of two steps(Fig. 4).

(1) (outer loop) Assuming the actuator is ideal, find the best force that will improve the suspension quality most.

(2) (inner loop) Taking the actuator dynamics into consideration, design a force controller that tracks the force command.

Though this procedure seems logical, the design procedure is complicated and there is no known way to optimize both the outer and inner loop control. That is, the overall performance depends highly on the capability of the chosen force controller.

The new single step controller in Fig. 5 no longer assumes the ideal actuator rather contains the actuator dynamics in the quarter car model. The controller is designed to improve the suspension performance only and does not care for the specific shape of the actuator force. The single step scheme which eliminates the unnecessary force control step is more understandable, and the analysis and control synthesis are made easier.

3.2 Optimal control design example

In this section to show the effectiveness of the modeling and control, the optimal state feedback control is employed as an example. All the state variables are assumed to be measurable and cost output is defined by

$$\mathbf{z_1} = [\, \ddot{z}_s \;\; z_s - z_u \;\; z_u - z_r \;\; \dot{z}_u \;\; f_a \;\; u \,]^T \tag{23}$$

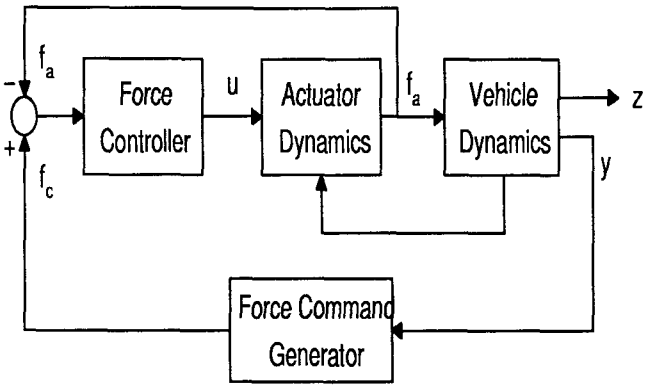

Fig. 4. Conventional control scheme

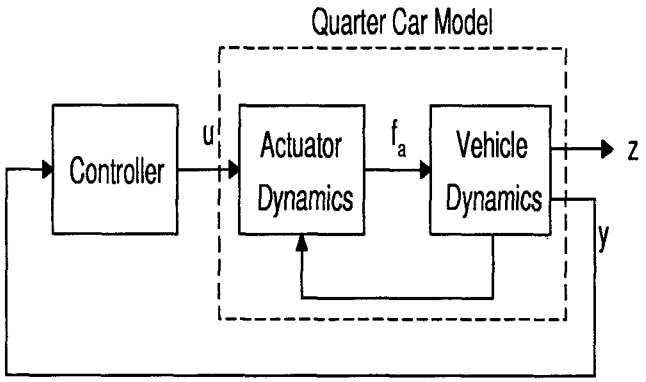

Fig. 5. New control scheme

$$= \begin{bmatrix} \mathbf{C_1 x} \\ u \end{bmatrix}$$

A linear quadratic cost functional is introduced to evaluate the quality of a suspension system.

$$J = \lim_{T\to\infty} \frac{1}{T} \int_0^T \begin{bmatrix} \mathbf{C_1 x} \\ u \end{bmatrix}^T \begin{bmatrix} \mathbf{Q}_{5\times5} & \mathbf{0}_{5\times1} \\ \mathbf{0}_{1\times5} & r \end{bmatrix} \begin{bmatrix} \mathbf{C_1 x} \\ u \end{bmatrix} dt$$

$$= \lim_{T\to\infty} \frac{1}{T} \int_0^T (q_1 \ddot{z}_s^2 + q_2 z_{su}^2 + q_3 z_{ur}^2 + q_4 \dot{z}_u^2 + q_5 f_a^2 + r u^2) dt \quad (24)$$

where $\mathbf{Q} = \mathrm{diag}[q_1, q_2, q_3, q_4, q_5], q_i \geq 0$, $(\sqrt{\mathbf{Q}}\mathbf{C_1}, \mathbf{A})$ is detectable and a scalar $r > 0$.
Then the control input which minimizes (24) is given as a state feedback

$$u = \mathbf{K x} \quad (25)$$

solving the corresponding algebraic riccati equation.

The true control input v, the voltage command to the servo valve, is calculated from (9), (25) with the measurement of the pressures p_1 and p_2.

$$v = q_s \times [K_{eq}(\sqrt{\Delta p_1} + \sqrt{\Delta p_2})]^{-1} = \mathbf{K x} \times [K_{eq}(\sqrt{\Delta p_1} + \sqrt{\Delta p_2})]^{-1} \quad (26)$$

The above conversion is always possible during the normal operation of actuator. The possible failure, when the piston hits either end of the cylinder, seldom occurs because an extra safety stroke is added normally in the hardware design phase.

3.3 Robust control against the uncertainty

The block diagram including the neglected uncertainty w_2 in (16) is shown in Fig. 4. The uncertainty output is defined by

$$\mathbf{z_2} = [\dot{z}_{su} \quad q_s]^T = \mathbf{C_2 x} \quad (27)$$

If the bounded parametric uncertainty block is defined by

$$\mathbf{\Delta} = [\delta_1 \quad \delta_2]_{1\times2} \quad (28)$$

Then the uncertainty w_2 is written by

$$w_2 = \mathbf{\Delta z_2} \quad (29)$$

With this model, we can apply well-known robust stability analysis, robust H^2 control design, and etc.

4. SIMULATION AND EXPERIMENT RESULTS

In this section the optimal controller is simulated and experimented. The model parameters listed below are based on the Quarter Car Test Rig at Postech.

Table 2. Test Rig parameter values

Symbol	Value	Unit
M_s	280	kg
M_u	50	kg
K_t	1.79×10^5	N/m
K_s	2.35×10^4	N/m
B_t	895	$N/m/s$
B_s	1500	$N/m/s$
K_{eq}	3.56	$m^{3.5}/kg^{0.5}/V$
P_s	$85 \times 10^5 a$	Pa
B	1.4×10^9	Pa
A_1	1.96×10^{-3}	m^2
A_2	1.35×10^{-3}	m^2
γ	1.4569	
L	160	mm
l_1, l_2	20	mm
$\hat{\alpha}$	4.636×10^7	kg/s^2
$\hat{\beta}$	1.4×10^10	$kg/s^2/m^2$

4.1 Simulation Results

$\mathbf{Q}$ and r in (24) are selected as

$$\mathbf{Q} = \mathrm{diga}[104.1, 3906.2, 62500, 1.0 \times 10^{-16}, 400], \quad r = 2.25 \times 10^8 \quad (30)$$

leading to the state feedback gain

$$\mathbf{K} = -[4166 \ 752 \ 8864 \ 1508 \ 2.43] \times 10^{-6} \quad (31)$$

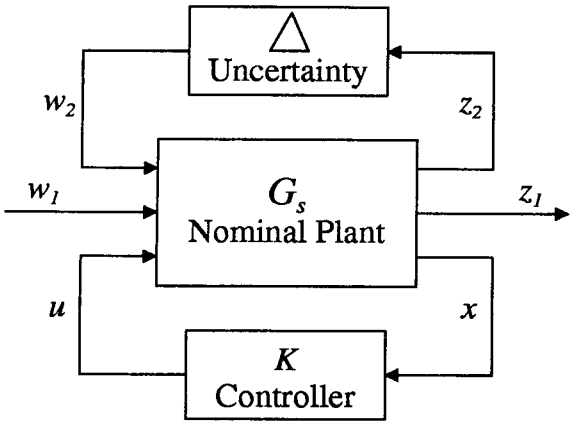

Fig. 6. Block diagram with an uncertainty

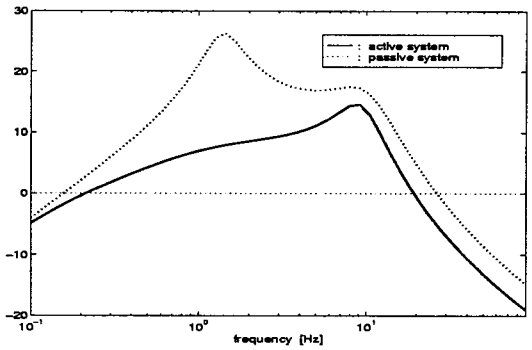

Fig. 7. Bode plot of $\frac{\ddot{z}_s}{\dot{z}_r}$

In selecting $\mathbf{Q}$ and r, focus is both on the ride quality(q_1) and the road holding(q_3). The resulting closed loop the bode plot of $\ddot{z}_s/\dot{z}_r$ is given Fig. 7. Although it is not easy to compare an active system without any passive elements with a passive system, the performance seems satisfactory.

To see the time response, a 2 Hz sinusoidal road disturbance with its amplitude $10mm$ is applied. In Fig. 8 (a) the amplitude of z_s is reduced to about $2mm$, and z_u tracks z_r well all the time. Fig. 8 (b) shows the our control input q_s and the corresponding v calculated by (26). As you see the plot of q_s is symmetric around 0, but that of v is not symmetric. Fig. 8 (c) shows the pressure p_i's and the force f_a. Note that the shape of the force command of two step scheme has surprisingly nothing common with that of actual force f_a. To see the effects of uncertainty $\delta(\cdot)$ the road amplitude is raised up to $40mm$ Then to enhance both the ride quality and the road holding, actuator stroke z_{su} is inevitably increased. However the resulting responses show little deviation from those of the nominal system. In Fig. 9 the plot of f_a is given and $|z_{su}|_\infty$ is $42.2mm$.

4.2 Experiment Results

Shaking experiments are performed on the Quarter Car Test Rig at Postech. The time responses of 1 Hz 15mm high road disturbance are shown in Fig. 10 and match well with the simulation results. The high frequency noise in Fig. 10 (b) indicates the existence of

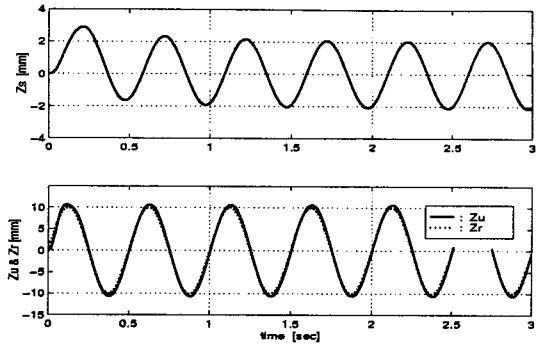

(a) Plot of z_s and z_u

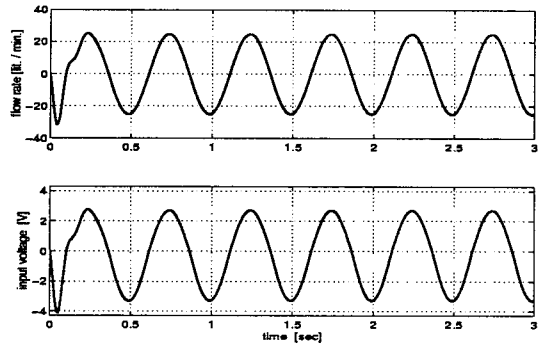

(b) Plot of q_s and u

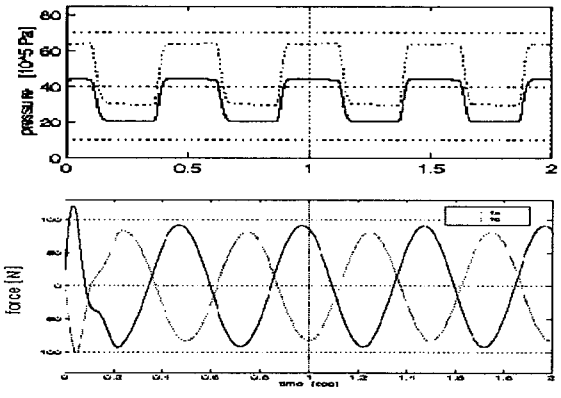

(c) Plot of p_i and f_a

Fig. 8. Time response to a 2 Hz sinusoidal road distur bance

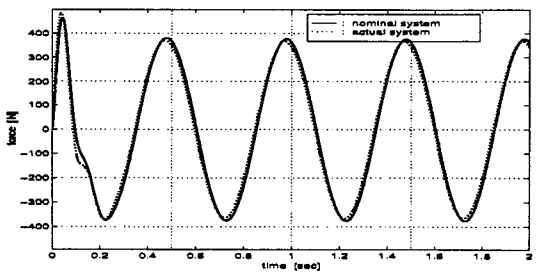

Fig. 9. Comparison of f_a with/without uncertainty

unmodeled dynamics which seems originated from the tire. The drift of pressure in (c) implies the leakage in the cylinder. To prevent the high frequency noise from destabilizing the system we filtered the calculated servo valve input in (d).

5. CONCLUDING REMARKS

In this paper we propose a new model and control for an automotive active suspension system. By considering the force as a state and the flow rate as an input, unnecessary force control step is eliminated and the analysis and synthesis are made quite easy. The simulation and experiment results support this point. Robust control methods are to be designed and tested by the test rig experiment to overcome the effects of the actuator uncertainty and the unmodeled high frequency dynamics.

6. REFERENCES

[1] C. Yue, T. Butsuen and J.K. Hedrick, "Alternative Control Law for Automotive Acive Suspensions", *J. of Dynamic Systems, Measurement, and Control, Trans. of the ASME*, **111**, pp.286-291, 1989.

[2] Y. Aoyama, K. Kawabata, S. Hasegawa, Y. Kobari, M. Sato and E. Tsuruta, "Development of the Full Active Suspension by Nissan", *SAE*, 901747, pp. 1537-1545, 1990.

[3] D. Hrovat, "Optimal Active Suspension Structures for Quarter-car Vehicle Models", *Automatica*, **26**, pp. 845-860, 1990.

[4] R.V. Dukkipati, M.O.M. Osman and S.S. Vallurupalli, "Adaptive active suspension to attain optimal performance and maintain static equilibrium level", *Int. J. of Vehicle Design*, **14**, pp. 471-496, 1989.

[5] P. Michelberger, L. Palkovics and J. Bokor, "Robust Design of Active Suspension System", *Int. J. of Vehicle Design*, **14**, pp. 145-165, 1993

[6] A.G. Thompson and P.M. Chaplin, "Force Control in Electrohyraulic Active Suspensions", *Vehicle System Dynamics*, **25**, pp. 185-202, 1996.

[7] A. Alleyne and J.K. Hedrick, "Nonlinear Adaptive Control of Active Suspensions", *IEEE Trans. Control Systems Technology*, **3**, pp. 94-101, 1995.

[8] H.E. Merritt, *Hydraulic Control Systems*, New York: Wiley, 1967.

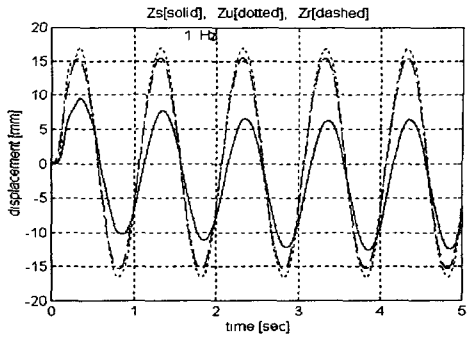

(a) Plot of z_s, z_u and z_r

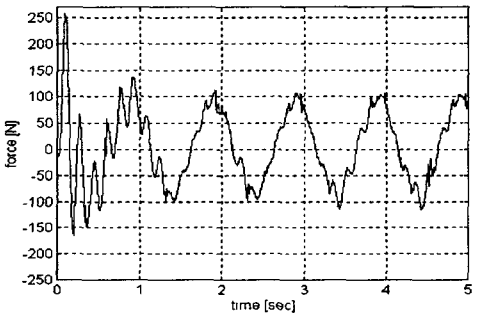

(b) Plot of f_a

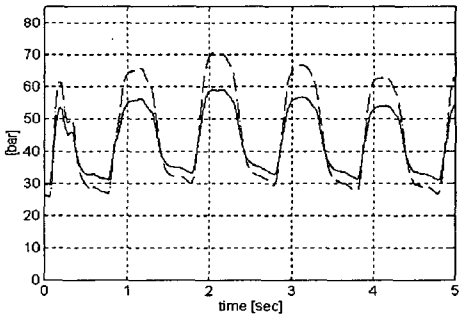

(c) Plot of p_1 and p_2

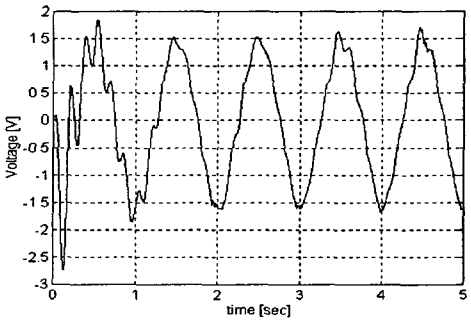

(d) Plot of v

Fig. 10. Time response to a 1 Hz sinusoidal road dis turbance